

Submitted to the Astrophysical Journal

**A Fit To The *Simultaneous* Broad Band Spectrum Of Cygnus X-1
Using The Transition Disk Model**

R. Misra

Inter-University Centre for Astronomy and Astrophysics, Pune, India

V. R. Chitnis

Tata Institute of Fundamental Research, Homi Bhabha Road, Mumbai, India.

Fulvio Melia¹

Department of Physics and Steward Observatory, University of Arizona, Tucson AZ

Received _____; accepted _____

¹Presidential Young Investigator.

ABSTRACT

We have used the transition disk model to fit the *simultaneous* broad band (2 – 500 keV) spectrum of Cygnus X-1 from OSSE and Ginga observations. In this model, the spectrum is produced by saturated Comptonization within the inner region of the accretion disk, where the temperature varies rapidly with radius. In an earlier attempt, we demonstrated the viability of this model by fitting the data from EXOSAT, XMPG balloon and OSSE observations, though these were not made simultaneously. Since the source is known to be variable, however, the results of this fit were not conclusive. In addition, since only once set of observations was used, the good agreement with the data could have been a chance occurrence. Here, we improve considerably upon our earlier analysis by considering *four* sets of *simultaneous* observations of Cygnus X-1, using an empirical model to obtain the disk temperature profile. The vertical structure is then obtained using this profile and we show that the analysis is self-consistent. We demonstrate conclusively that the transition disk spectrum is a better fit to the observations than that predicted by the soft photon Comptonization model. In particular, although the transition disk model has only one additional parameter, the χ^2 value is reduced and there are no systematic residuals. Since the temperature profile is obtained by fitting the data, the unknown viscosity mechanism need not be specified. The disk structure can then be used to infer the viscosity parameter α , which appears to vary with radius and luminosity. This behavior can be understood if α depends intrinsically on the local parameters such as density, height and temperature. However, due to uncertainties in the radiative transfer, quantitative statements regarding the variation of α cannot yet be made.

Subject headings: accretion disks—black hole physics—radiation mechanisms:
thermal—relativity—stars: Cygnus X-1

1. Introduction

During the last two decades, the X-ray/ γ -ray spectrum of Cygnus X-1 has been extensively studied by, e.g., HEAO1, EXOSAT, Ginga and the Compton GRO. This black hole system settles into two distinct long term configurations, namely the so-called soft and hard states. In the hard state, the X-ray spectrum is dominated by 2 – 200 keV emission, which has been interpreted by some to be the result of the inverse Compton scattering of cold external photons by a hot ($kT \approx 50$ keV) low density plasma. This plasma could be the innermost region of the accretion disk (Shapiro, Lightman & Eardley 1976), or it could be a corona overlying a relatively cold disk (Liang & Price 1977; Haardt & Maraschi 1993). An alternative model is one in which the emission is a sum of multi-temperature Wien peaks from the transition region of the disk (Maraschi & Molendi 1990; Misra & Melia 1996). All these models predict a similar spectrum which is more or less a power-law with an exponential cutoff.

However, it may now be possible to differentiate between these models by combining the data from various high-energy instruments, such as OSSE, Ginga and EXOSAT, and thereby studying the broad band nature of this source. The initial steps in this direction were taken by Chitnis, Rao & Agrawal (1997) and Gierlinski et al. (1997). They concluded that a simple soft-photon Comptonization model does not adequately fit the data. Instead, significant systematic residuals were obtained, and it appeared that an additional *ad hoc* spectral component is needed to account for the observations. Gierlinski et al. (1997) have also pointed out that the spectrum is photon starved which argues against an overlying coronal model in which roughly half of the radiated high-energy photons are reflected back into the emitting region by the cold disk.

Subsequently, Misra et al. (1997) showed that the transition disk model (Misra & Melia 1996) appears to fit the broad band data without invoking an additional component.

In this picture, the structure of the accretion disk is obtained without assuming *a priori* that the effective optical depth in the vertical direction is much greater than unity. This leads to an electron temperature that varies rapidly with radius (Maraschi & Molendi 1990; Misra & Melia 1996), and the spectrum differs in a significant way from a simple power-law with an exponential cut off. This spectrum fits the data well and is not associated with any systematic residuals. These results indicated that the transition disk model may be a better fit to the observations than the spectrum expected from a single temperature external photon Comptonization.

However, the earlier analysis by Misra et al. (1997) used non-simultaneous observations by EXOSAT, XMPC balloon flights and OSSE. Since the source is known to be variable, the results of this analysis were not conclusive. Moreover, since only one set of observations was used, it was not clear whether the agreement with the transition model was a chance occurrence. An additional complication was the fact that a direct χ^2 comparison between the transition disk and soft photon Comptonization models could not be made since the latter was not fit to the same data. It was shown only that the transition model did not produce any systematic residuals whereas the Comptonization model (fit to a different data set) did give rise to these.

In this paper, we use four sets of simultaneous observations of Cygnus X-1 made with Ginga and OSSE. These data have already been analyzed with an isotropic Comptonization model by Gierlinski et al. (1997). Here, we reanalyze the data using the transition disk model and compare our results with those of the previous study. Following Misra et al. (1997) we fit the data to an empirical model instead of making a direct fit to the more complicated exact equations. The best fit temperature profile is then used to determine the disk structure. In the final step, the viscosity parameter α is inferred from the disk structure.

In the next section, we briefly describe the empirical model developed by Misra et al. (1997). In §3 the observations and the results of the spectral fit to the transition model are compared with those obtained by Gierlinski et al. (1997). In §4 we calculate the disk structure from the best fit temperature profile and we discuss the self-consistency of our analysis. §5 summarizes the basic results.

2. The Empirical Model

To keep the calculation tractable, we use an empirical model developed by Misra et al. (1997) to fit the data, rather than attempt a solution of the full equations. We emphasize that the difference between the transition disk model and the empirical model is in the parametrization. Instead of the physical parameters such as the mass accretion rate, the black hole mass and the viscosity parameter α , we use empirical parameters like the temperature profile and the absolute normalization described below.

The gravitational energy released per unit area for each side of the disk is (Shakura & Sunyaev 1973)

$$F_g = \frac{3}{8\pi} \frac{GM\dot{M}}{R^3} J(R), \quad (1)$$

where $J(R) = 1 - (R_i/R)^{1/2}$ and R_i is the radius of the last stable orbit, here taken to be $R_i = 3R_g$, with $R_g \equiv 2GM/c^2$. We assume that the temperature profile of the disk is given by

$$\theta \equiv kT = 0.1 \left(\frac{r}{r_o} \right)^n J^m \text{ keV}. \quad (2)$$

where r_o is the radius of the disk at which $\theta = 0.1 J^m \approx 0.1$ keV. Using this profile and assuming *a priori* (but checked later for self-consistency) that the radiative mechanism is saturated Comptonization (i.e., a Wien peak), we obtain the flux at earth (Misra et al.

1997):

$$f_E(E) = KE^2 \int_0^{r_o} (\theta)^{-4} \exp(-E/\theta) r^{-2} dr \quad \text{photons/sec/cm}^2/\text{keV} , \quad (3)$$

where E is the photon energy in keV and

$$K = 5.59 \times 10^{27} \dot{M} D^{-2} , \quad (4)$$

where D is the distance to the source. This intrinsic spectrum is a function of K , n , m , and r_o .

To this must be added a reflection component, which has been calculated using the appropriate Green's function (White, Lightman, & Zdziarski 1988), under the assumption that the reflecting medium is neutral and averaging over incident and observing angles. The reflected component depends only on the intrinsic spectrum and the solid angle subtended by the reflector, which is conveniently normalized by the factor $R_{ref} = \Omega/2\pi$. Here $R_{ref} = 1$ would correspond to an angle averaged reflection spectrum due to a reflector which suspends a solid angle 2π with respect to the X-ray source. Since the reflected spectrum depends on the incident and observing angles, the real solid angle could be different from the best fit R_{ref} which is treated here like a parameter. It should be noted that the shape of the reflected spectrum taking into account the angle of observation is similar to the angle averaged one, however there could be a difference in normalization (Magdziarz & Zdziarski 1995). Together with the earlier four parameters, the quantity R_{ref} renders the final spectrum (which is used to fit the data) a function of five independent parameters.

Since the temperature profile of the transition region is obtained in this way, the unknown viscosity mechanism does not need to be specified in order for us to obtain the disk structure. In principle, the disk equations can be inverted and the viscosity parameter (α) can then be obtained as a function of radius. As shown by Misra et al. (1997), however, this has only a limited value since the inferred α strongly depends on the details of the vertical radiative transfer. Here, we show that this is still the case, but since there are now

four sets of data, it is possible to infer some useful qualitative trends. We will see that α is a function of radius and luminosity, which may be understood in the context of its intrinsic dependence on the local parameters such as density, height and temperature.

3. Observations and Results

Ginga observed Cygnus X-1 on several occasions, one of which was 1991 June 6, during the OSSE viewing period 2. Gierlinski et al. (1997) have extracted four Ginga (2 – 30 keV) data sets from this period and the corresponding near simultaneous OSSE observations to perform their spectral fit. We are using the same set of observations for the present study. A systematic error of 1% is included in each of the Ginga channels.

The OSSE data span the energy range from 50 to 1000 keV, and systematic errors are included. These are computed from the uncertainties in the low energy calibration and response of the detectors, using in-orbit and prelaunch calibration data. The energy-dependent systematic errors are expressed as an uncertainty in the effective area in the OSSE response and are added in quadrature to the statistical errors. They are most important at the lowest energies, contributing an approximate 3% uncertainty in effective area at 50 keV, decreasing to 0.3% at 150 keV and above. The details of these observations are given in Table 1 of Gierlinski et al. (1997).

We fit the four sets of data using the empirical model described in the previous section. Following Gierlinski et al. (1997), we consider only data above 3 keV, so that the soft X-ray excess does not effect the fitting. The relative normalization between Ginga and OSSE is allowed to vary freely within ± 15 per cent. In all four cases, the best fit normalization falls within this range. The spectrum is absorbed by a line of sight column density using the cross section given in Morrison & McCammon (1983). A lower limit of $5 \times 10^{21} \text{ cm}^{-2}$,

corresponding to galactic absorption, is imposed on all the optimizations. This is consistent with ASCA measurements by Ebisawa et al. (1996). We model the iron line as a Gaussian, whose centroid energy is restricted to lie within the range 6.3 – 6.6 keV and whose line width is 0.1 – 0.2 keV, consistent with the ASCA measurements (Ebisawa et al. 1996).

Table 1 summarizes the results of our spectral fits. The χ^2 in each case is comparable to or smaller than those obtained by Gierlinski et al. (1997), who used a single temperature isotropic external photon Comptonization model. We show in Figure 1 the unfolded spectrum and the residuals for set 1. Unlike the single temperature model, there are no strong systematic residuals and hence a second component is not required here. Similar results were obtained for the other three data sets. This solidly establishes the results indicated earlier by Misra et al. (1997), who used non-simultaneous data. The spectral parameters (i.e., n , m and r_o) are similar for all four data sets, which suggests that the spectral shape does not vary strongly with luminosity, as was also pointed out by Gierlinski et al. (1997).

To check the robustness of these results we have re-fitted the data after fixing $n = -3.5$, which is different from the best fit value $n \approx -2.5$. The ensuing results are shown in Table 2. Evidently, the χ^2 increased by about ~ 10 , but the reduced χ^2 is still ~ 1 and thus a temperature profile corresponding to this set of parameters cannot be excluded. As we note in the next section, these two sets of parameters give rise to different disk structures. However, since the $\Delta\chi^2$ is large, the latter case should be considered an extreme case.

4. The transition disk

Using the best fit empirical temperature profile obtained in the previous section, we can now derive the physical structure of the disk, subject to a number of assumptions.

Table 1: Spectral parameters for the transition disk model

| Model | Parameters | set-1 | set-2 | set-3 | set-4 |
|----------------|--------------------------------|------------------|------------------|------------------|------------------|
| component | | | | | |
| abs | N_H (10^{22} cm $^{-2}$) | 0.5 | 0.57 ± 0.22 | $1.25 \pm .22$ | $1.1 \pm .22$ |
| Gaussian | E_{Line} (keV) | 6.38 ± 0.1 | 6.44 ± 0.1 | 6.43 ± 0.11 | 6.31 ± 0.21 |
| | σ (keV) | 0.2 | 0.2 | 0.2 | 0.2 |
| | K_{Line} | 9.06 ± 1.6 | 10.0 ± 1.7 | 5.59 ± 1.0 | 4.32 ± 1.3 |
| | EW (eV) | 124 | 126 | 115 | 93.3 |
| transit | r_o | 114.9 ± 15.5 | 109.4 ± 10.3 | 155.9 ± 26.6 | 96.0 ± 17.6 |
| | n | -2.50 ± 0.16 | -2.62 ± 0.24 | -2.18 ± 0.16 | -2.71 ± 0.25 |
| | m | 0.87 ± 0.12 | 1.03 ± 0.18 | 0.62 ± 0.11 | 0.98 ± 0.2 |
| | R_{ref} | 0.642 ± 0.06 | 0.644 ± 0.07 | 0.39 ± 0.06 | 0.513 ± 0.07 |
| | K | 46.8 ± 0.61 | 54.0 ± 0.9 | 32.75 ± 0.4 | 29.98 ± 0.88 |
| | K_{osse} | $0.92 \pm .02$ | $0.89 \pm .02$ | 0.99 ± 0.02 | $0.97 \pm .04$ |
| χ^2 (dof) | | 58.96 (75) | 67.33 (75) | 60.59 (75) | 63.52 (75) |

¹The normalization constants for the Gaussian line is in units of 10^{-3} photons cm $^{-2}$ s $^{-1}$.

K_{osse} : Normalization of the OSSE spectrum relative to the Ginga spectrum.

Table 2: Spectral parameters for the transition disk model with frozen $n = -3.5$

| Model | Parameters | set-1 | set-2 | set-3 | set-4 |
|----------------|--------------------------------|------------------|------------------|------------------|------------------|
| component | | | | | |
| abs | N_H (10^{22} cm $^{-2}$) | 1.18 ± 0.10 | 1.09 ± 0.1 | 2.27 ± 0.1 | 1.55 ± 0.10 |
| Gaussian | E_{Line} (keV) | 6.49 ± 0.14 | 6.56 ± 0.15 | 6.6 | 6.39 ± 0.17 |
| | σ (keV) | 0.2 | 0.2 | 0.2 | 0.2 |
| | K_{Line} | 6.5 ± 1.3 | 7.9 ± 1.5 | 3.0 ± 0.8 | 3.1 ± 0.8 |
| | EW (eV) | 88 | 97.5 | 60 | 65 |
| transit | r_o | 63.43 ± 1.8 | 67.13 ± 2.1 | 63.35 ± 1.9 | 64.2 ± 3.7 |
| | n | -3.5 | -3.5 | -3.5 | -3.5 |
| | m | 1.54 ± 0.07 | 1.69 ± 0.08 | 1.51 ± 0.07 | 1.59 ± 0.14 |
| | R_{ref} | 0.849 ± 0.04 | 0.807 ± 0.04 | 0.702 ± 0.03 | 0.62 ± 0.06 |
| | K | 50.2 ± 0.6 | 57.5 ± 0.7 | 35.38 ± 0.4 | 32.19 ± 0.68 |
| | K_{osse} | $0.91 \pm .02$ | $0.87 \pm .02$ | 0.96 ± 0.02 | $0.93 \pm .04$ |
| χ^2 (dof) | | 71.85 (76) | 72.99 (76) | 83.54 (76) | 67.65 (76) |

¹The normalization constants for the Gaussian line is in units of 10^{-3} photons cm $^{-2}$ s $^{-1}$.

K_{osse} : Normalization of the OSSE spectrum relative to the Ginga spectrum.

The procedure was developed in detail by Misra et al. (1997), so we provide only a brief summary here.

The assumptions that will be checked for self-consistency are 1) that the plasma cools via saturated bremsstrahlung self-Comptonization and 2) that advection is not important. The structure equations are those for hydrostatic equilibrium, the radiative transfer and radiative cooling. These equations, together with Equation (1), completely determine the disk structure with the use of the best fit temperature profile. Note that the torque equation generally used in standard disk solutions is not needed here, since the necessary information is contained in the temperature profile. Thus the unknown viscosity process does not need to be specified in this scheme. The handling of the radiative transfer is the most uncertain among these equations and is accounted for with the expression

$$F_g = B_1 \frac{cP_r}{\tau} , \quad (5)$$

where F_g is the energy flux, P_r is the radiation pressure and τ is the scattering optical depth. The uncertainty is represented by the factor B_1 , which is taken to be of order unity. In the radiative cooling equation, the bremsstrahlung rate is multiplied by the Compton Amplification factor (Svensson 1983). Using the proton electron Coulomb energy transfer we take into account the possibility that the proton temperature may be different from that of the electrons. The total pressure is taken to be the sum of the radiation and gas pressures.

The normalization parameter K (Eq. 4) may be directly related to the mass accretion rate (Misra et al. 1997):

$$\dot{M} = 5.3 \times 10^{17} \left(\frac{K}{50} \right) \left(\frac{D}{2.5 \text{kpc}} \right)^2 \text{ grams/sec} . \quad (6)$$

We take the distance to the source to be 2.5 kpc and assume that the black hole mass is ten solar masses.

In Figure 2, we show the variation of temperature, scattering optical depth and pressure with radius for set 1, in which $B_1 = 0.25$. These disk characteristics are qualitatively similar to those inferred earlier by Misra et al. (1997). In Figure 3, the effective optical depth τ_{eff} is plotted as a function of radius (appearing in the lower right hand corner). In the same plot, the Compton y parameter $y \equiv (4kT_e/m_e c^2)\tau^2$ is shown as a function of radius. The fact that $\tau_{eff} < 1$ and $y \sim 1$ justifies the assumption that the radiative mechanism is Comptonized bremsstrahlung. To check the self-consistency of our second assumption (regarding the insignificance of advection), we have also calculated the ratio of the pressure to the number density times the virial temperature ($\approx m_p c^2/r$):

$$P_a/P = \frac{\rho c^2}{r} \frac{1}{P}, \quad (7)$$

and have plotted it in Figure 3. Since this ratio is always much greater than one, advection is not important and the disk is geometrically thin. Analogous self-consistency checks have been carried out for the other three observational sets as well.

Following Misra et al. (1997), we have next calculated the viscosity parameter α as a function of radius from the inverted disk equations. Figure 4 shows this quantity corresponding to the first data set for two values of B_1 and n . Clearly, α depends rather strongly on the actual value of B_1 , and hence the radiative transfer, as may be inferred from a comparison of the solid and dotted curves in this figure. It also depends in an important way on n , as may be seen by inspecting the dashed curve in Figure 4. Since the data do not discriminate strongly among the variations of α with radius, it is difficult to make concrete statements about the viscosity based on these results.

Nonetheless, with four sets of data corresponding to different luminosities, it is still possible to discern qualitative trends. Figure 5 shows the variation of α with radius for the best fit temperature profile in each of the four data sets (solid curves). The viscosity parameter α seems to vary inversely with the luminosity, which itself scales with the

accretion rate. However, α should in principle depend only on local parameters such as height, density and temperature. We have found that the following empirical “fit” for α in terms of these parameters, reproduces the variation quite well:

$$\alpha(\Xi, T) = 2.65 \left(\frac{T}{10^8 \text{K}} \right)^{-0.85} \left(\frac{\Xi}{10 \text{ g cm}^{-2}} \right)^{-2.8}, \quad (8)$$

where Ξ is the column density. This empirical fit is shown (dotted curve) in Figure 5. Care should be taken when interpreting this result since α depends sensitively on the uncertainty in the radiative transfer. Moreover, the fit itself may not be unique. We are showing this here primarily to demonstrate that it is possible to obtain a functional form for α that depends only on the local parameters.

5. Summary

We have produced a fit to four sets of simultaneous broad band data for Cygnus X-1 within the context of the transition disk model. These data were obtained with observations by OSSE (50 – 500 keV) and Ginga (3 – 30 keV). We have established rather strongly that the transition disk model fits the data better than a pure soft-photon Comptonization model, as suggested earlier by Misra et al. (1997) based on non-simultaneous data. In particular the χ^2 value for the transition disk model is in each case smaller than or comparable to that of the isotropic Comptonization model fit to the same data (Gierlinski et al. 1997). In addition, unlike the soft-photon Comptonization model, there are no systematic residuals for the transition disk fit. The transition disk is described by four parameters as compared to the isotropic Comptonization model which has three. However, for the model presented here no additional ad hoc component, with two extra parameters (Gierlinski et al. 1997) are needed.

We have also determined the disk structure from the best fit temperature profiles, and

through self-consistency checks, we showed that our initial assumptions were valid. The viscosity parameter α inferred from the calculated disk structure was found to depend on the details of the vertical radiative transfer and the spectral fitting. Thus, it is not yet possible to make concrete statements regarding its value or specific tendencies. However, since we were able to analyze the data at four different epochs (each corresponding to a different luminosity), we derived the qualitative variation of α with radius and luminosity, which we accounted for in terms of its dependence on the local disk structure parameters, such as density, temperature and height.

The authors thank A. A. Zdziarski and M. Gierlinski for providing us with the reduced data from OSSE and Ginga. RM and VRC thank A. Kembhavi for useful discussions. VRC acknowledges IUCAA for its hospitality. This work was partially supported by NASA grant NAG 5-3075.

REFERENCES

- Chitnis, V., Rao, A.R. & Agrawal, P.C., 1997, *Astr. Ap.*, submitted.
- Ebisawa, K., Ueda, Y., Inoue, H., Tanaka, Y. & White, N.E., 1996, *ApJ*, **467**, 419.
- Gierlinski et al., 1997, *MNRAS*, **288** 958.
- Haardt, F. & Maraschi, L., 1993, *ApJ*, **413**, 507.
- Liang, E.P. & Price, R.H., 1977, *ApJ*, **218**, 247.
- Magdziarz, P. & Zdziarski A.A. 1995, *MNRAS*, **273**, 837.
- Maraschi, L. & Molendi, S., 1990, *ApJ*, **353**, 452.
- Misra, R. & Melia, F., 1996, *ApJ*, **467**, 405.
- Misra, R., Chitnis, V., Melia, F. & Rao, A.R., 1997, *ApJ*, *in press*
- Morrison, R. & McCammon, D., 1983, *ApJ*, **270**, 119.
- Shakura, N.I. & Sunyaev, R.A. 1973, *Astr. Ap.*, **24**, 337.
- Shapiro, S.L., Lightman A.P. & Eardley, D.M. 1976, *ApJ*, **204**, 187.
- Svensson, R. 1983, *MNRAS*, **209**, 175.
- White, T.R., Lightman, A.P. & Zdziarski, A.A. , 1988, *ApJ*, **331**, 939.

Fig. 1.— The deconvolved spectrum of Cygnus X-1 corresponding to the first data set, obtained from simultaneous observations with Ginga and OSSE. The contributions from individual model components, viz., the iron line and reflection, are shown separately. The residuals to the model fit are shown in the lower panel as a contribution to the χ^2 .

Fig. 2.— (a) The temperature profile in the disk for the best fit values in data set 1, and $B_1 = 0.25$. Solid curve: electron temperature; dotted curve: proton temperature. (b) The scattering optical depth ($\tau = n_p \sigma_T H$) as a function of radius corresponding to the temperature profile in (a) and $B_1 = 0.25$. (c) The mass density as a function of radius corresponding to the temperature profile in (a) and $B_1 = 0.25$. (d) Pressure as a function of radius corresponding to the temperature profile in (a) and $B_1 = 0.25$. Solid curve: Radiation pressure; Dotted curve: Gas pressure.

Fig. 3.— The effective optical depth (τ_{eff}), the Compton y parameter and the ratio P_a/P as functions of radius for data set 1.

Fig. 4.— The viscosity parameter α as a function of radius for data set 1. Solid curve: $B_1 = 0.25$; Dashed curve: $B_1 = 0.5$. The dotted curve is for a temperature profile calculated with $n = -3.5$.

Fig. 5.— The viscosity parameter α (solid curve) as a function of radius for data sets 1, 2, 3, and 4. Dotted curve: empirical fit given by Equation (8) in the text.

Figure 1

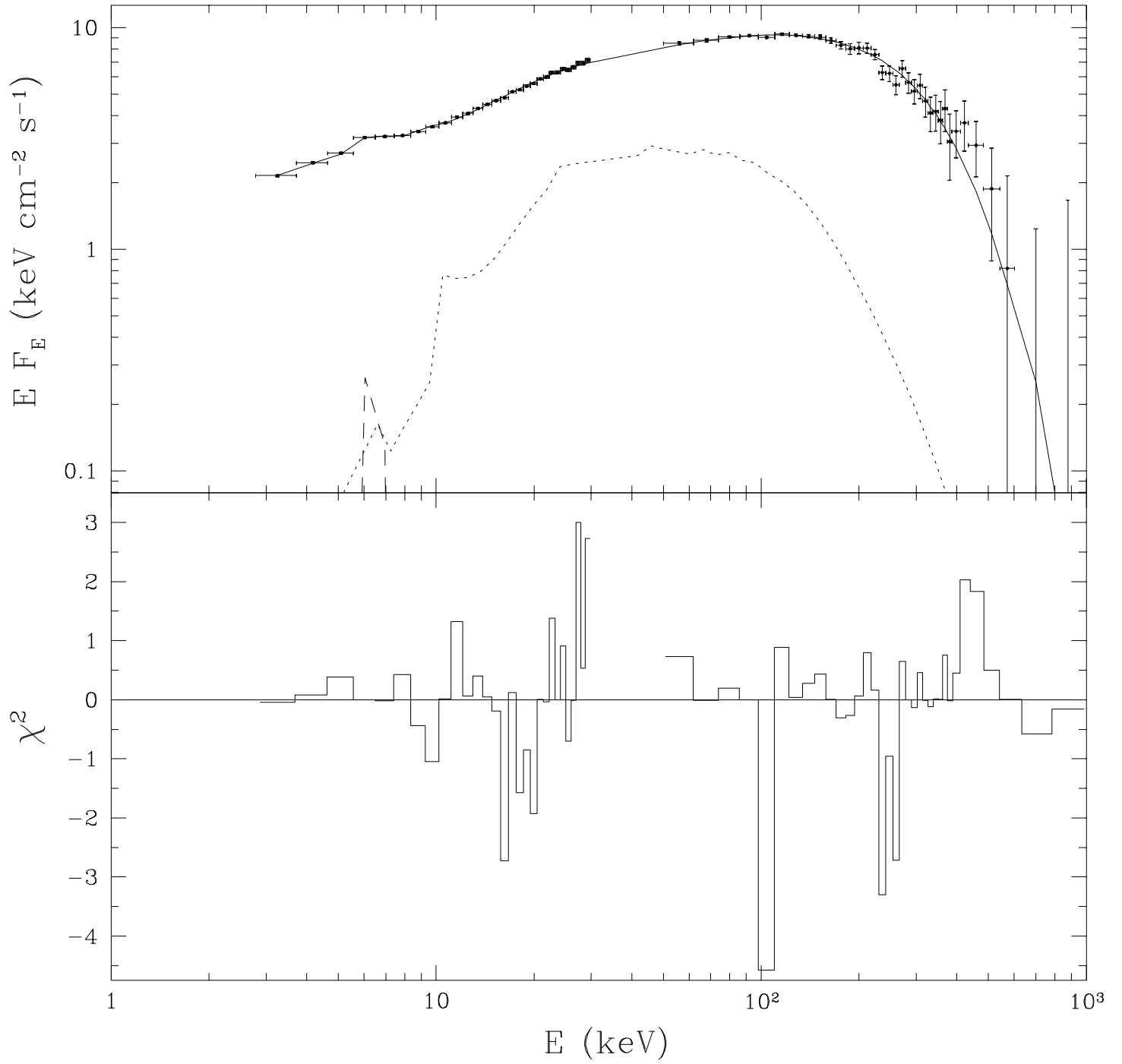


Figure 2 (a)

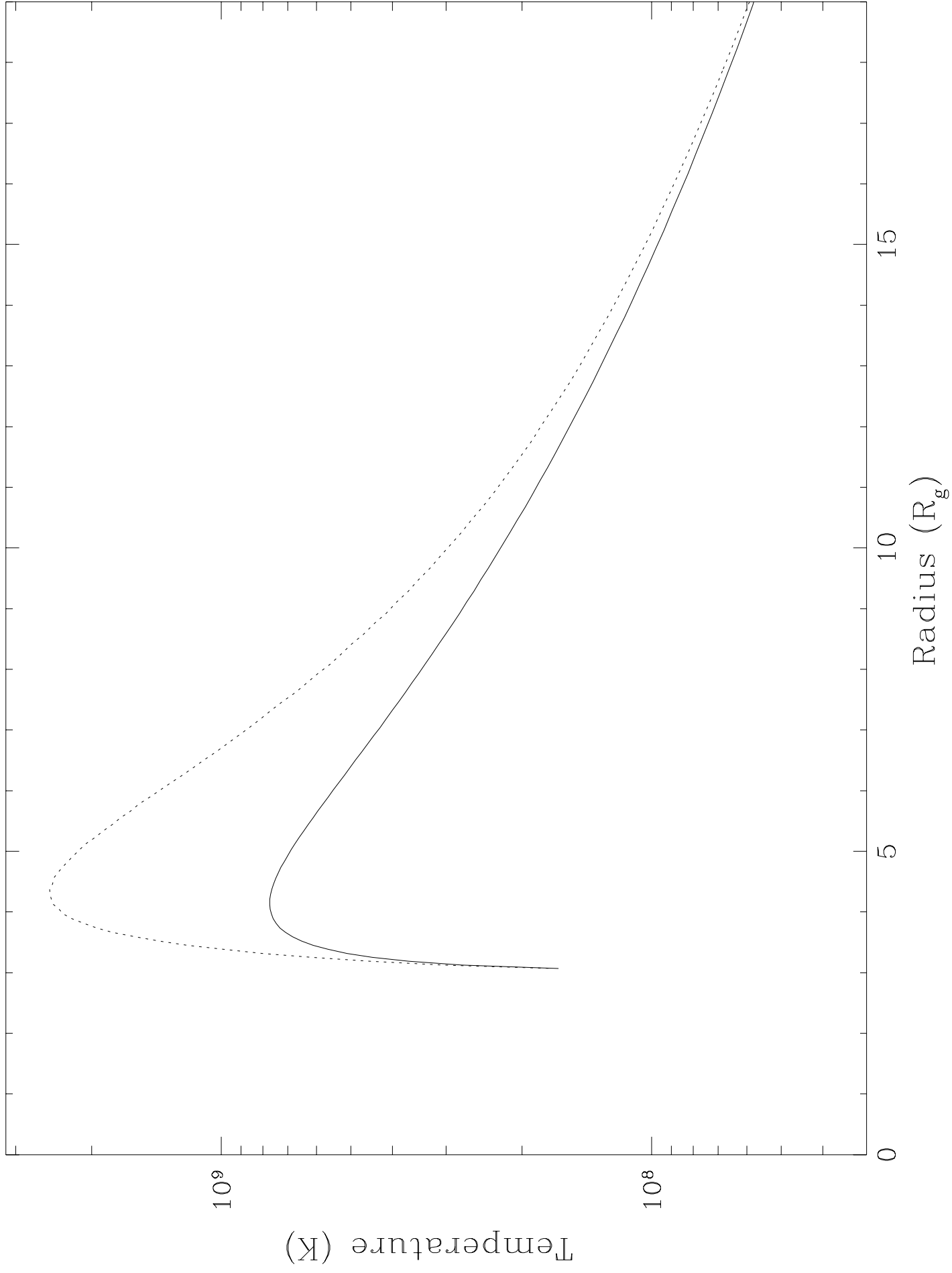


Figure 2 (b)

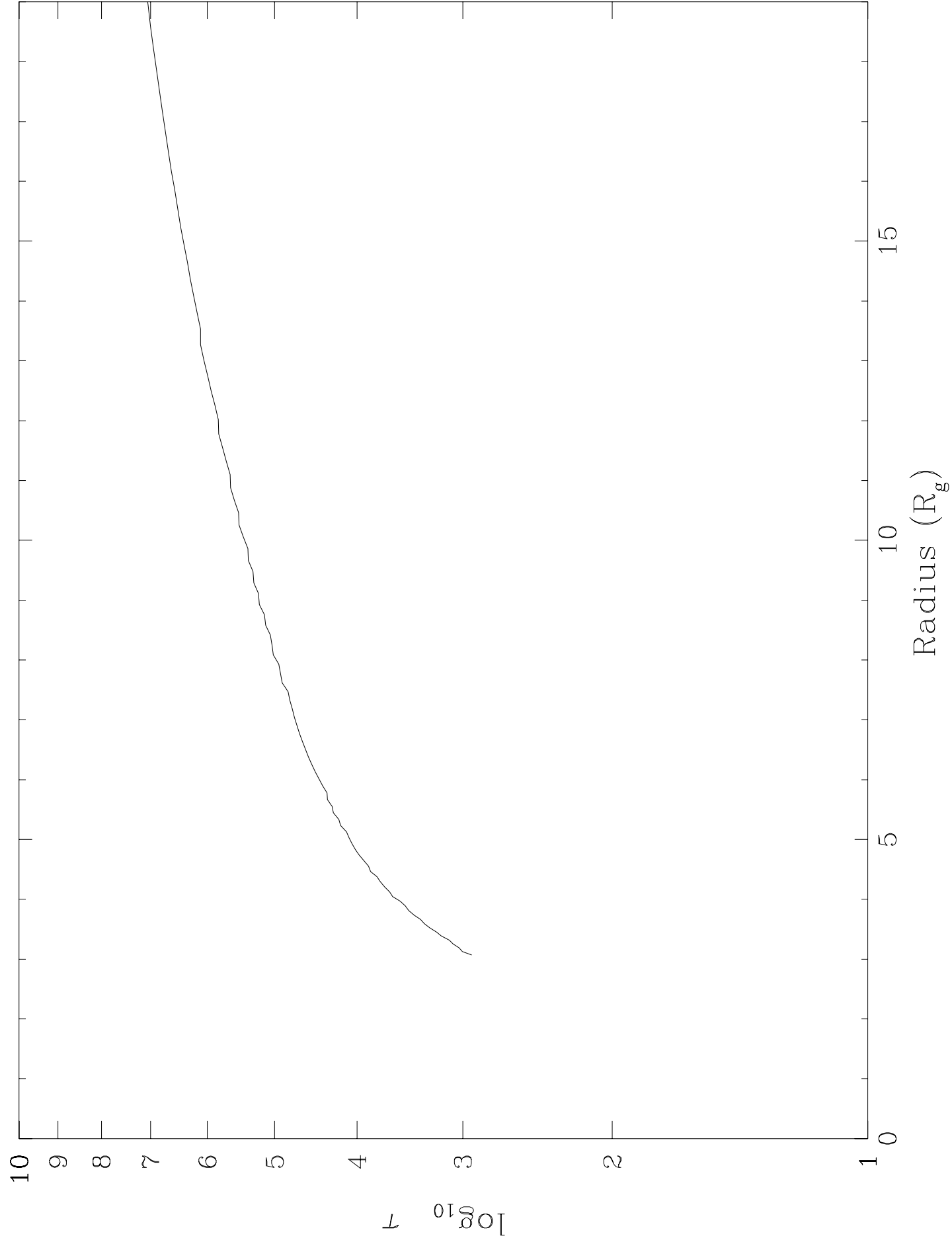


Figure 2 (c)

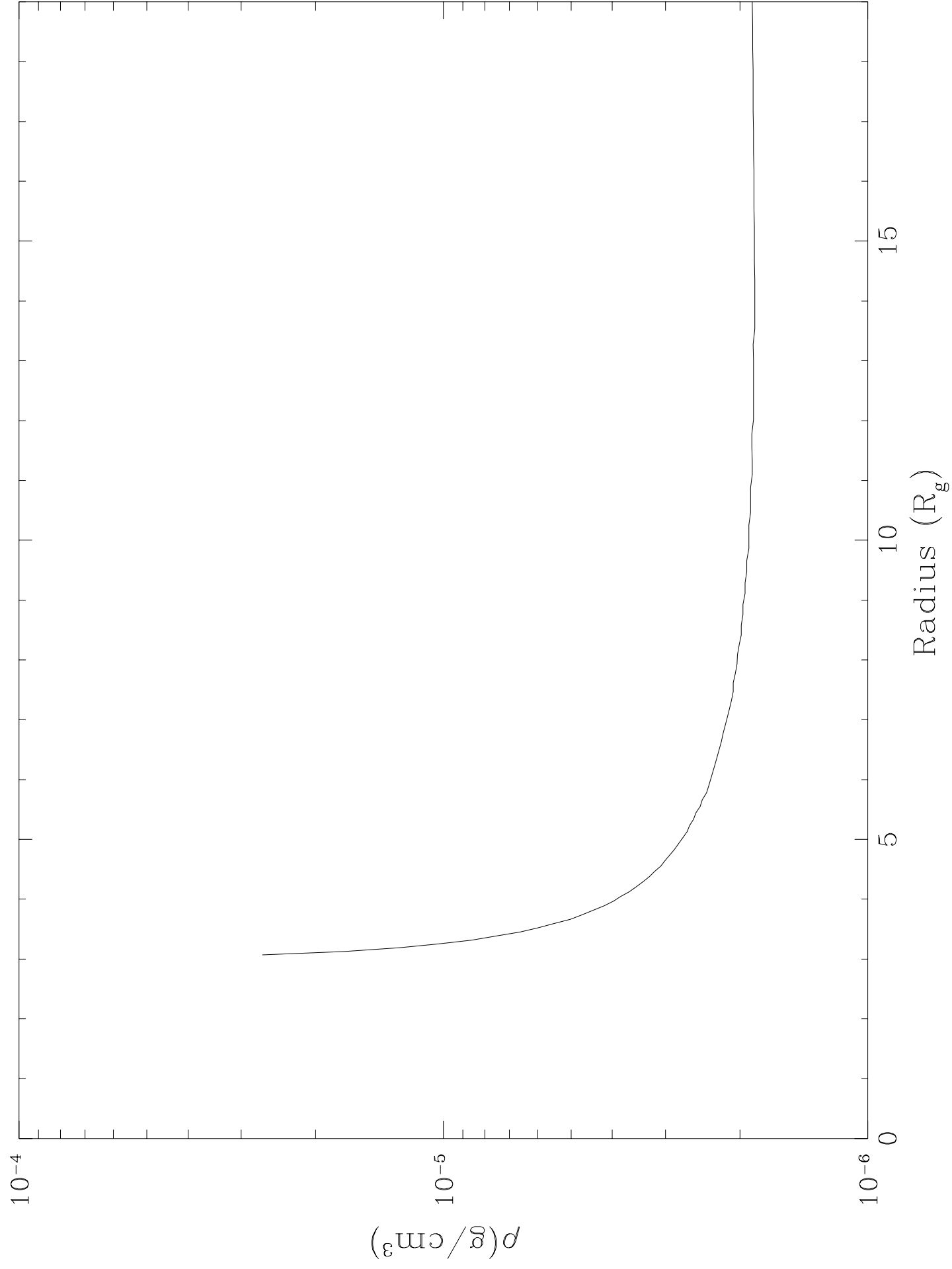


Figure 2 (d)

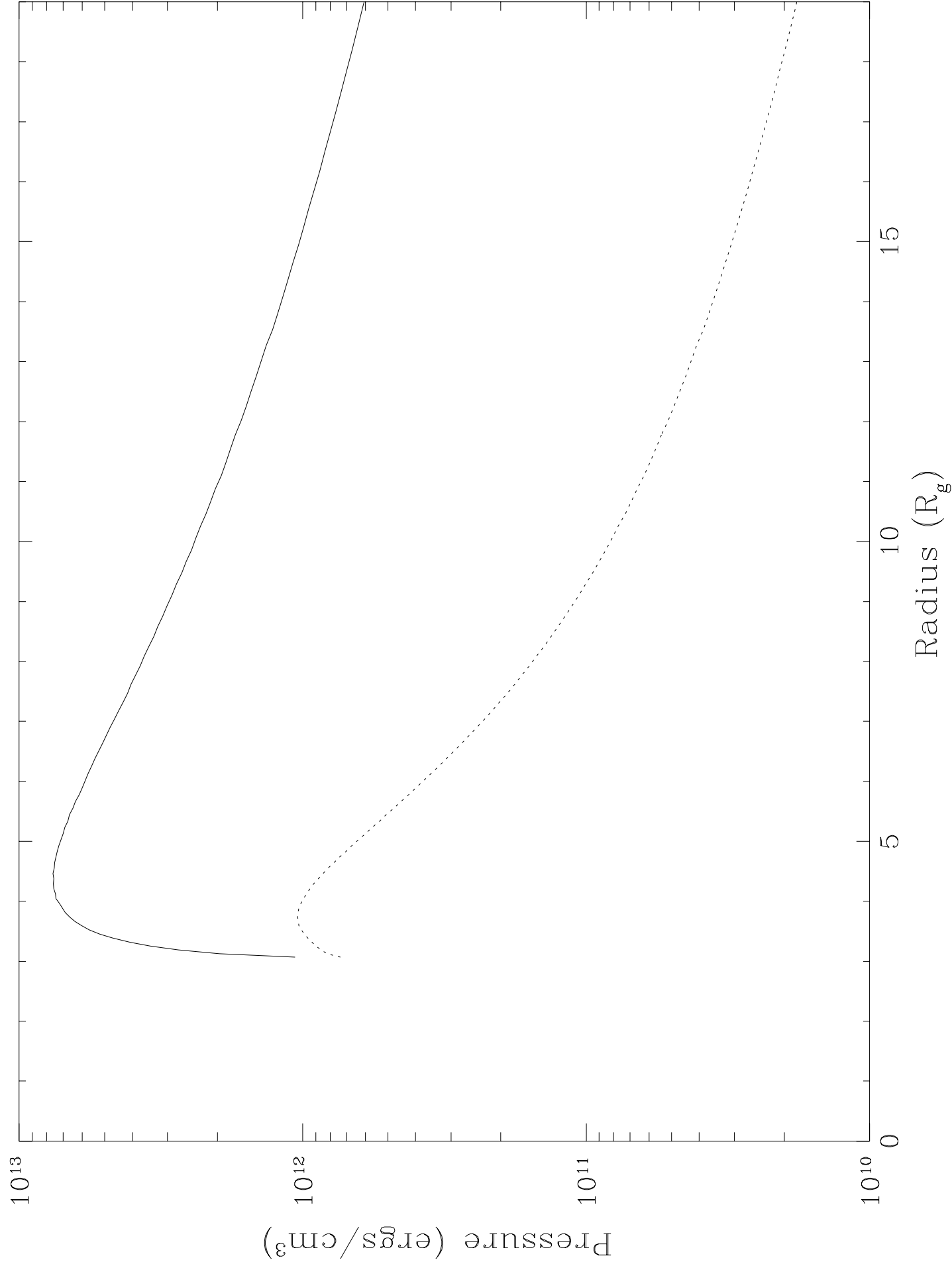


Figure 3

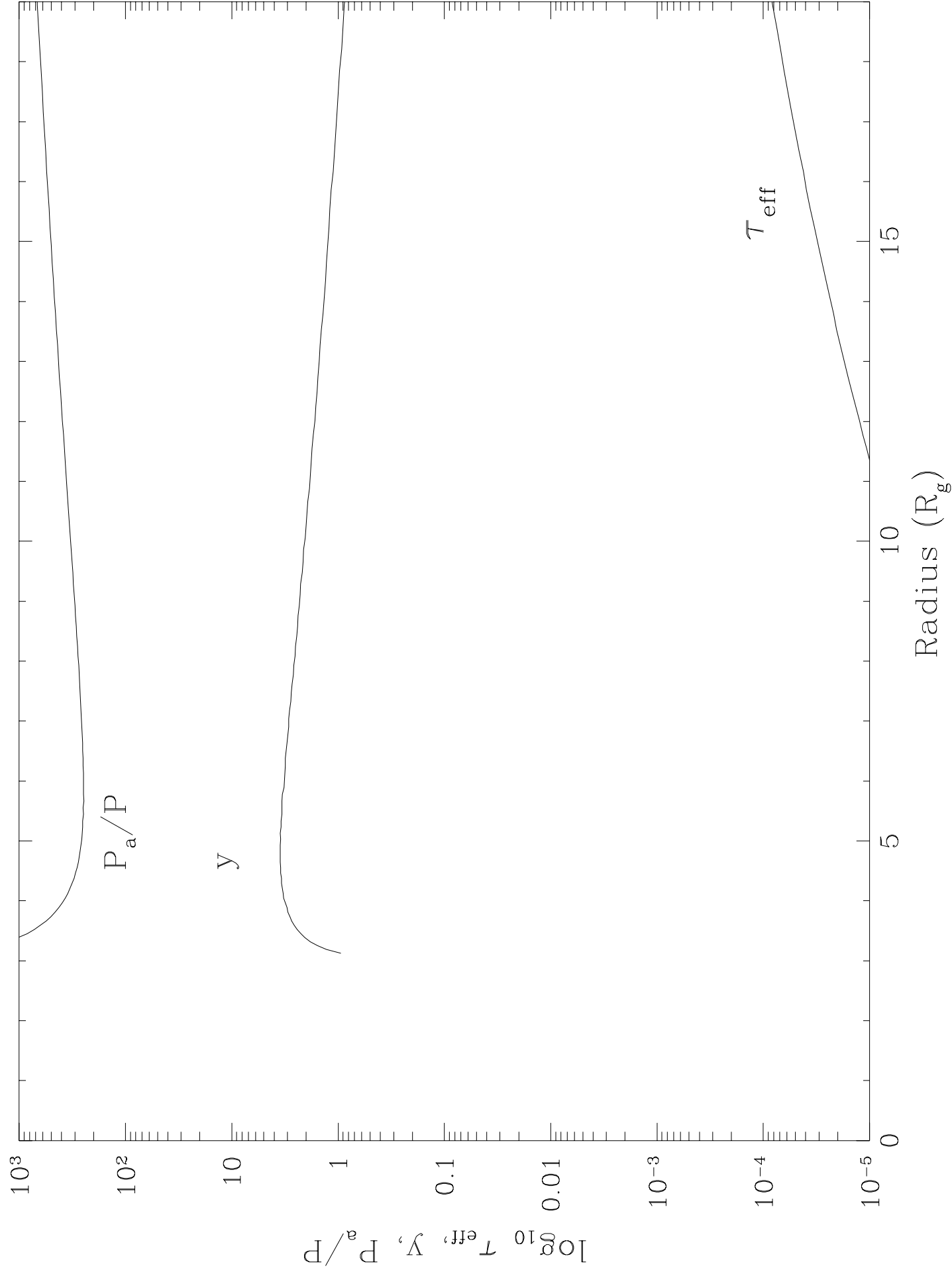


Figure 4

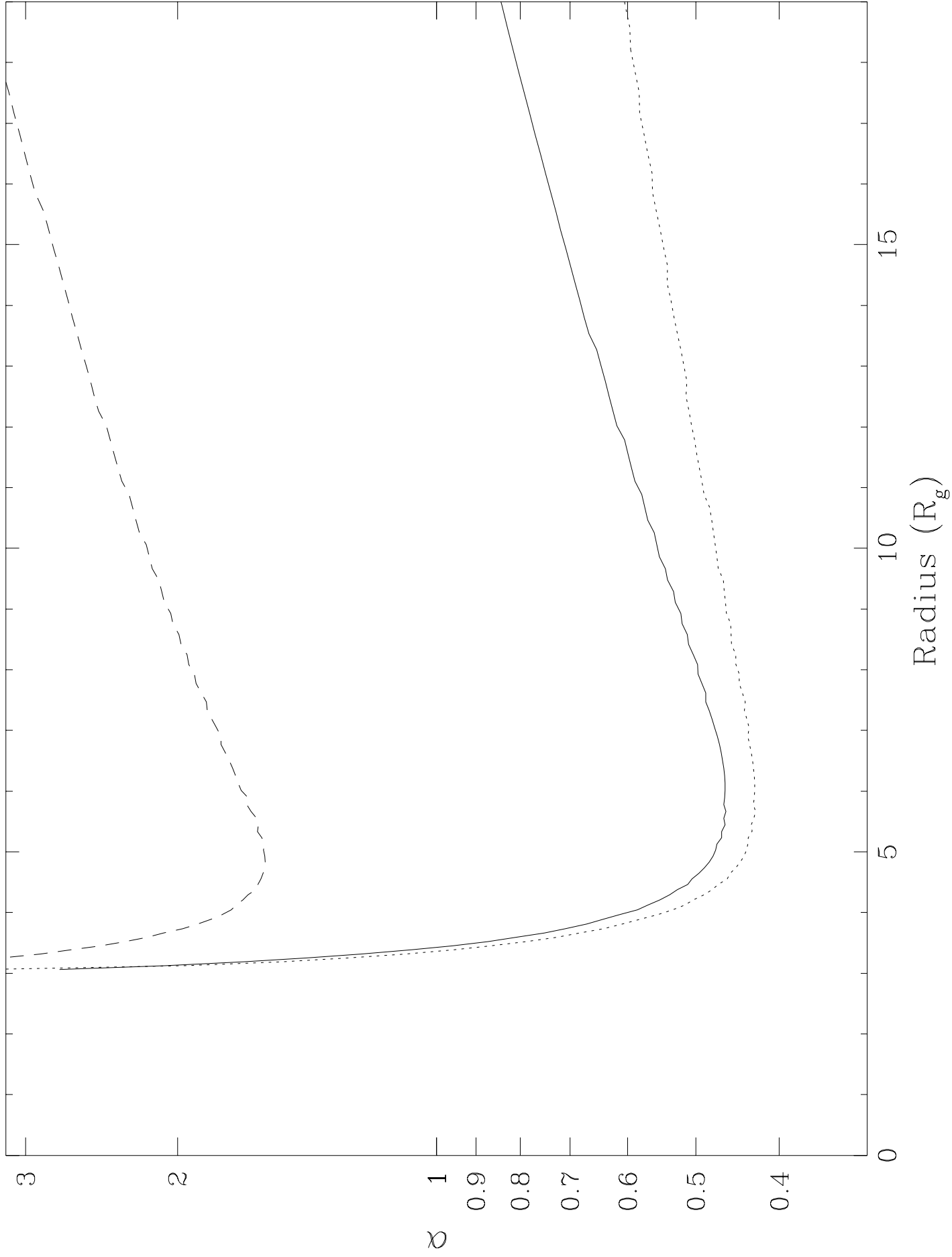


Figure 5

